

Next generation long baseline experiments on the path to leptonic CP violation

P. M igliozzi^{a;1} and F. Terranova^{b;2}

^a INFN, Sezione di Napoli, Naples, Italy

^b INFN, Laboratori Nazionali di Frascati, Frascati (Rome), Italy

Abstract

In this paper we quantify the trade-off between setups optimized to be ancillary to Phase II Superbeams or Neutrino Factories and experiments tuned for maximal sensitivity to the subdominant terms of the neutrino transition probability at the atmospheric scale ("maximum discovery potential"). In particular, the ν_{13} sensitivity is computed for both Phase I superbeams (JHF-SK and NuMI O-Axis) and next generation long baseline experiments (ICARUS, OPERA and MINOS). It is shown that Phase I experiments cannot reach a sensitivity able to ground (or discourage in a definitive manner) the building of Phase II projects and that this capability is almost saturated by high energy beams like CNGS, especially for high values of the ratio m_{21}^2/m_{31}^2 .

PACS: 14.60.Pq, 14.60.Lm

¹pasquale.migliozzi@cern.ch

²francesco.terranova@cern.ch

1 Introduction

The possibility to perform a CKM-like precision physics in the leptonic sector employing terrestrial neutrino oscillation experiments has been deeply debated in the last few years. At present, the occurrence of neutrino oscillations seems rather well established [1, 2, 3]. Current experimental evidence indicates two hierarchical mass scale differences ($m_{21}^2 \neq m_{32}^2 \neq m_{31}^2$) driving, respectively, the oscillations at the "solar" and "atmospheric" scale. Moreover, the $m_{21}^2 = m_{31}^2$ ratio is constrained by the LMA solution of the solar neutrino puzzle to lie between 0 (0:1) and 0 (0:01) [4]. If this scenario will be confirmed after the completion of ongoing experiments (K2K [2], KAM-LAND [3] and MINIBOONE [5]) and next generation long baseline projects (MINOS [6], ICARUS [7], OPERA [8]), terrestrial neutrino experiments based on "Superbeam" (SB) or "Neutrino Factories" (NF) could be the ideal tool for precision measurements of the PMNS [9] leptonic mixing matrix and the discovery of leptonic CP violation [10]. These experiments explore subdominant effects in the neutrino transition probabilities at the atmospheric scale which, in general, are suppressed by at least one power of $\sin^2 \theta_{13}$. Hence, the recent KAMLAND result places SB and NF proposals on a firmer ground since guarantees that subdominant effects will not be suppressed to an unobservable level ($\sin^2 \theta_{13} < 10^{-2}$). This condition, however, is not enough to establish the physics reach of SB/NF. As for the case of CKM physics, CP violating effects depend on the size of the Jarlskog invariant [11]. In the standard parameterization [12] of the PMNS matrix this coefficient can be expressed as:

$$J = \frac{1}{8} \sin 2\theta_{12} \sin 2\theta_{23} \sin 2\theta_{13} c_{13} \sin \theta_{13} \quad (1)$$

where $s_{ij} = \sin \theta_{ij}$ and $c_{ij} = \cos \theta_{ij}$. Differently from the quark case, the leptonic Jarlskog invariant is enhanced by the large mixing angles θ_{23} and θ_{12} . On the other hand, due to the null result of the CHOOZ [13] and PALO VERDE [14] experiments, the full three-flavor mixing of neutrinos is still unestablished and only upper limits on the $\sin^2 \theta_{13}$ parameter have been drawn ($\sin^2 \theta_{13} < 0 (10^{-1})$). Moreover, no theoretical inputs are available to constrain the size of θ_{13} in a convincing manner, so that its experimental determination is mandatory. The discovery of $\theta_{13} \neq 0$ has not only a scientific relevance but also a high practical value. The commissioning and running of an apparatus to observe CP violation in the leptonic sector at the atmospheric scale (e.g. JHF-Phase II or a Neutrino Factory) is a major technical and economical challenge; since most of its physics reach – in particular the measurement of leptonic CP violation and the determination of U_{e3} in the PMNS matrix – depends crucially on the size of θ_{13} , the latter should be determined by "Phase I" experiments (e.g. JHF-SK [15] or NuMI 0-Axis [16]) tuned to maximize their θ_{13} sensitivity. Otherwise, the physics case of SB/NF should be drawn independently of their PMNS reach. This is marginally possible for JHF-Phase II (proton decay with HyperK) but rather unrealistic for NF. The physics case of Phase I experiments is very appealing due to their

unprecedented precision in the determination of the parameters leading the oscillations at the atmospheric scale ($_{23}$ and $j m_{31}^2$) and their significant discovery potential for high values of $_{13}$. On the other hand, the sensitivity of Phase I experiments to $_{13}$ has been questioned since a significant deterioration is expected once we account for our complete ignorance of the leptonic CP phase, the sign of m_{31}^2 and the $_{23}$ ambiguity [17, 18]. In this context, the advantage of a 'pure' $_{13}$ measurement has been put forward especially in connection with new reactor experiments [19].

In this letter we quantify the trade-off between a setup optimized to be ancillary with respect the SB/NF project (maximum $_{13}$ sensitivity) and one highly sensitive to the subdominant terms of the transition probability (maximum discovery potential). In particular, we challenge the claim that a Phase I experiment can reach a sensitivity able to ground (or discourage in a definitive manner) the building of SB/NF and show that this capability is almost saturated by first generation long baseline experiments like CNGS.

2 Oscillation probabilities

The next generation long baseline experiments (MINOS, ICARUS and OPERA) and Phase I experiments (JHF-SK and NuMIO-Axis) employ baselines in the 300–700 km range. In most of the cases, the neutrino energy is optimized to maximize the oscillation probability at the atmospheric scale for the corresponding baseline (hE i' 0.7–3 GeV). The CNGS experiments, however, make use of a high energy beam, well beyond the kinematic threshold for production (hE i' 17 GeV). The main parameters for the setups under consideration are listed in Table 1. In all cases the subleading oscillations at the solar scale are suppressed by at least one order of magnitude compared with the atmospheric ones. Hence, oscillation probabilities can be expanded in the small parameters and $\sin 2_{13}$. The inclusion of matter effects is simplified here, since the earth density can be considered constant along baselines shorter than 1000 km. In particular, the ν_e oscillation probability can be expressed as [20, 21]:

$$\begin{aligned}
 P_{\nu_e \rightarrow \nu_e} = & \sin^2 2_{13} \sin^2 2_{23} \frac{\sin^2 [(1 - \hat{A})]}{(1 - \hat{A})^2} \\
 & \sin 2_{13} \sin \theta \sin(\phi) \frac{\sin(\hat{A})}{\hat{A}} \frac{\sin [(1 - \hat{A})]}{(1 - \hat{A})} \\
 & + \sin 2_{13} \cos \theta \cos(\phi) \frac{\sin(\hat{A})}{\hat{A}} \frac{\sin [(1 - \hat{A})]}{(1 - \hat{A})} \\
 & + \cos^2 2_{23} \sin^2 2_{12} \frac{\sin^2(\hat{A})}{\hat{A}^2}
 \end{aligned}$$

$$O_1 + O_2(\theta) + O_3(\theta) + O_4 : \quad (2)$$

In this formula $m_{31}^2 L = (4E)$ and the term s contributing to the Jarlskog invariant are split into the small parameter $\sin 2_{13}$, the $O(1)$ term $\cos_{13} \sin 2_{12} \sin 2_{23}$ and the CP term $\sin \theta \hat{A}^2 2G_F n_e E = m_{31}^2$ with G_F the Fermi coupling constant and n_e the electron density in matter. Note that the sign of \hat{A} depends on the sign of m_{31}^2 which is positive (negative) for normal (inverted) hierarchy of neutrino masses. The dominant contributions among the four terms $O_1 \dots O_4$ of Eq. 2 are determined by the choice of L and E . In the following, if not stated explicitly, we assume the present best fits for the solar and atmospheric parameters ($m_{21}^2 = 7.3 \times 10^5$ eV², $\sin^2 2_{12} = 0.8$, $m_{31}^2 = 2.5 \times 10^3$ eV², $\sin^2 2_{23} = 1$) [4]³.

	JHF-SK	NumIOA	M INOS	ICARUS	OPERA
Baseline (km)	295	712	735	732	732
Mean energy (GeV)	0.76	2.22	3	17	17
Exposure (kton years)	22.5 5	17 5	5.4 2	2.4 5	1.7 5
L/E (km /GeV)	388	321	245	43	43

Table 1: Main parameters of the Phase I and long baseline experiments.

JHF-SK

JHF-SK has been tuned to maximize the discovery potential and subdominant contributions depending on the CP phase are enhanced. Given its short baseline matter effects represent a small correction to the oscillation probability ($\hat{A}' \approx 5 \times 10^2$). Assuming an average neutrino energy of 0.76 GeV, the following hierarchy among the terms of Eq. 2 is obtained:

$$P_{\nu_e \nu_e} \approx \sin^2 2_{13} A_1 \sin \theta \sin 2_{13} A_2 + \cos \theta \sin 2_{13} \cos(\theta) A_3 + A_4^2 \quad (3)$$

where the A_i ($i = 1, \dots, 4$) coefficients are $O(1)$. The actual values of the terms contributing to Eq. 2 are shown in Fig. 1. Here, the θ -depending terms O_2 and O_3 are computed at maximum amplitude, $O_2(\theta = \pi/2) = O_3(\theta = 0)$, to illustrate the impact of assuming complete ignorance on θ in the extraction of $\sin^2 2_{13}$. Of course, in the oscillation probability formula when O_2 (O_3) is maximal, i.e. $\theta = \pi/2$ ($\theta = 0$), the other coefficient O_3 (O_2) is zero. For $\sin^2 2_{13}$ sufficiently high:

$$P_{\nu_e \nu_e} \approx \sin 2_{13} (\sin 2_{13} A_1 \sin \theta A_2) \quad (4)$$

³For $\sin^2 2_{13} \approx 4$ other degenerate solutions appear at $\theta = 0$ [22].

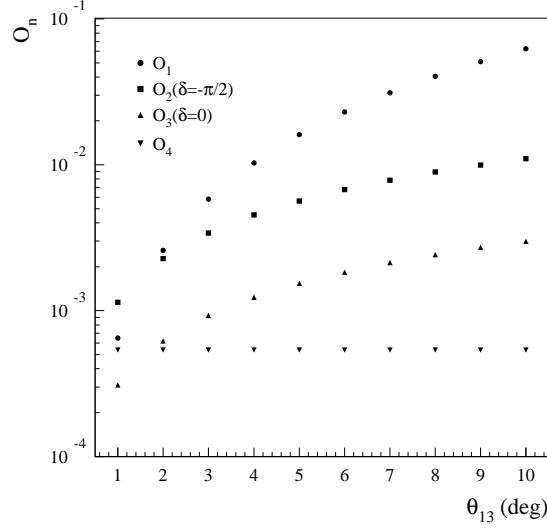


Figure 1: Contribution of the $O_1 \dots O_4$ terms to the oscillation probability in the JHF-SK scenario.

Eq. 3 and 4 show that the deterioration of the $\sin^2 2 \theta_{13}$ sensitivity coming from the θ_{13} -ambiguity [23] is strictly connected to the mass scale ratio θ_{13} . Hence, the maximum sensitivity is achieved in the limit $\theta_{13} \rightarrow 0$ which corresponds to minimum sensitivity to the subdominant terms of $P_{\nu_{13}}$ (minimum discovery potential). Clearly, this contradictory request is at the origin of the conflict between setups ancillary to SB/NF and experiments able to explore a significant fraction of the PMNS parameter space. For JHF-SK, the deterioration effect becomes sizable already at $\theta_{13} \approx 3^\circ$ (see Fig. 1). Values of θ_{13} higher than the ones assumed in Fig. 1 ($\theta_{13} > 0.03$) imply earlier appearance of the (θ_{13}) deterioration effect.

Note that Eq. 3 cannot be used in a straightforward manner to extract the actual sensitivity of a Phase I experiment. The signal rate is:

$$S = Y A \frac{Z}{dE} (\bar{E}) P_{\nu_{13}} (\bar{E}) (\bar{E}) (\bar{E}) \quad (5)$$

where \bar{E} is the flux at the surface of the detector, A is proportional to the detector mass, Y are the years of data taking and $P_{\nu_{13}} (\bar{E})$ is the production cross-section weighted with the detection efficiency for the ν_e CC final state. The signal rate is proportional to $P_{\nu_{13}} (\bar{E})$ only in the narrow band limit $\bar{E} \approx \bar{E}_0$ ($\bar{E} \ll \bar{E}_0$). The minimum accessible probability P_{\min} depends on the background rate and it has to be computed through a full simulation. We further address this issue in Sec. 3. Finally, note that for P_{\min} sufficiently low ("Phase II" measurements), setups can be envisaged to lift explicitly the θ_{13} ambiguity, e.g. combining different baselines [24] or different oscillation channels [25] or building a single baseline experiment with a

detector capable of observing more than one oscillation peak [26].

NuM IO -Axis and MINOS

The NuM IO -Axis proposal envisages the possibility of getting a very narrow beam placing a dedicated detector for e appearance (20 kton, low-Z calorimeter) at an angle of 0.7° with respect to the present NuM I axis. Again, L and E are tuned close to the first oscillation maximum at the atmospheric scale. A significant reduction of the background coming from NC with 0 production can be reached, compared with the MINOS setup, thanks to the suppression of the high energy tail of the beam. Once more, the terms contributing to Eq. 2 keeps the form of Eq. 3 with A_i ($i = 1, \dots, 4$) ranging between 0.4 and 0.6. However, both MINOS and NuM IO -Axis employ a baseline of ~ 700 km and matter effects are sizable ($\Delta \sim 0.2$) in this regime since they modify the size of the leading term A_1 . As a consequence, these setups offer a significant sensitivity to the sign of m_{31}^2 . On the other hand, if it is not possible to disentangle the sign (m_{31}^2) degeneracy from the effect proportional to $\sin^2 2_{13}$, an additional source of deterioration of the $\sin^2 2_{13}$ sensitivity appears. In principle, it could be possible to re-tune NuM IO -Axis releasing the condition $\mu = 2$ and, hence, modifying the relative weights of the A_i coefficients. In this scenario, NuM I would be complementary to JHF-SK since the former would lower its bare $\sin^2 2_{13}$ sensitivity allowing the latter to relieve the ($\sin^2 2_{13}$) deterioration discussed above. This possibility and the overall improvement in the PMNS reach of the synergic JHF/NuM I physics program have been discussed in details in [17, 19] and will not be further considered here.

CNGS

The CNGS beam has been tuned to reach maximum sensitivity to the e appearance channel. To overcome the limitation of the high threshold for ν production, the condition $\mu = 2$ has been given up and $\mu_{CNGS} \sim 0 (10^1)$. As a consequence, the oscillation probability is suppressed by the damping term $\sim 10^{-2}$,

$$P(\bar{\nu}_e \rightarrow \bar{\nu}_e) \sim \cos^4 2_{13} \sin^2 2_{23}^{-2} \quad (6)$$

but the event rate profits of the high e -CC cross-section. The same damping factor limits the search for $\bar{\nu}_e \rightarrow \bar{\nu}_e$. Again, this loss of signal events is partially compensated by the linear rise of the e -CC cross-section and by the high granularity of the corresponding detectors tuned for e (in particular $\bar{\nu}_e \rightarrow e$) appearance and hence, extremely effective in suppressing the NC (0) and $\bar{\nu}_e \rightarrow \bar{\nu}_e$ background. It has been shown [27] that ICARUS and OPERA combined could explore the region down to $\sin^2 2_{13} \sim 0.025$ at $\sin^2 m_{31}^2 \sim 2.5 \times 10^{-3}$ eV^2 and assuming 6.75×10^{19} pot/year. The analysis is dominated by the statistical fluctuations of the e beam contamination from

K_{e3} decays and, for higher exposure time, by the systematic uncertainty on its overall normalization⁴ (see Fig. 6 in Section 3). However, this analysis does not include the deterioration effect coming from the CP phase and the sign of m_{31}^2 . In principle, matter effects should be even higher than NuMI because \hat{A} grows linearly with E and the two setups have the same baseline ($\hat{A}' = 1.6$). However, since $j(1 - \hat{A}) \approx 1$, we get:

$$\frac{\sin^2[(1 - \hat{A})]}{(1 - \hat{A})^2}, \quad (7)$$

and the leading term A_1 turns out to be unaffected by the sign of m_{31}^2 . Eq. 2 reads now:

$$P_{\pi^+ e^-} \stackrel{h}{\sim} \sin^2 2_{13} A_1 \sin \sin 2_{13} A_2 + \cos \sin 2_{13} A_3 + \frac{1}{2} A_4^2 \quad (8)$$

and, again, $A_1 \dots A_4$ are O(1) coefficients, albeit different from the ones of Eq. 3. The values of the terms contributing to Eq. 2 at CNGS are shown in Fig. 2. The overall scale is suppressed by $\frac{1}{2}$ and the role of the O_2 and O_3 terms are exchanged w.r.t. JHF due to the different size of \sin and \cos . Here, O_3 is responsible for the ($\sin 2_{13}$) deterioration effect which is sizable in the same 2_{13} region as for JHF. Note, however, that O_3 (O_2) is odd (even) under the transformation $m_{31}^2 \rightarrow -m_{31}^2$; so, at CNGS, going from normal to inverted hierarchy has the same effect of performing a $\pi^+ e^-$ transformation in the CP phase. Note also that both JHF-SK and CNGS see a deterioration of their sensitivity to 2_{13} starting from the 3° region (or before for higher θ).

3 Numerical calculations

Analyses of the $\pi^+ e^-$ channel in the leading order approximation $P(\pi^+ e^-) \approx O_1$ have been published by the collaborations involved in the Phase I and next generation long baseline experiments. Hence, it is possible to make a reliable estimation of the actual sensitivities side-stepping the full simulation of the various setups. The condition that excludes a point $(\sin^2 2_{13}; m_{31}^2)$ of the parameter space at a given confidence level, once the null hypothesis $\sin^2 2_{13} = 0$ has been experimentally observed and a given value of α is assumed, is

$$\chi^2(\sin^2 2_{13}; m_{31}^2) > \quad (9)$$

where

⁴The CNGS physics program m_e does not foresee the construction of a near detector.

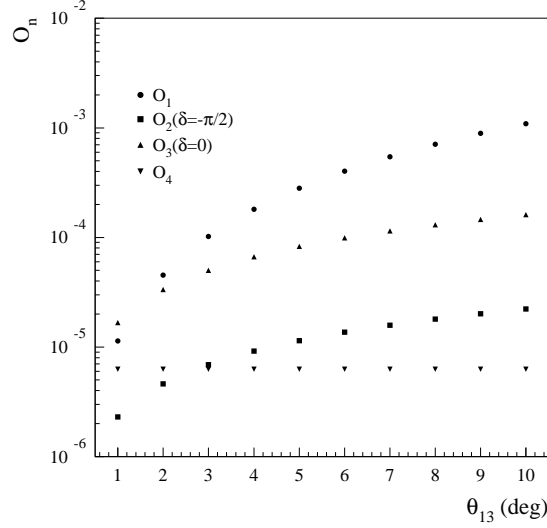


Figure 2: Contribution of the $O_1 \dots O_4$ terms to the oscillation probability at CNGS.

$$\begin{aligned}
 & \frac{R^{\text{th}}}{R^{\text{obs}}} = \\
 & \frac{h}{\frac{(S(\sin^2 2_{13}; m_{31}^2) + B)}{S_{\text{null}} + B + \frac{2}{2} B^2}} > \frac{(S_{\text{null}} + B)^{i_2}}{(S_{\text{null}} + B)^{i_2}} \quad (10)
 \end{aligned}$$

In this formula, which holds in Gaussian approximation, R^{th} is the expected ν_e rate for the current value of $(\sin^2 2_{13}; m_{31}^2)$ and R^{obs} is the rate corresponding to the null hypothesis. Eq. 2 shows that the null hypothesis is independent of the CP phase and the sign of m_{31}^2 and depends only on $|m_{31}^2|$. S and B represent the signal and background rate, h is the systematic uncertainty on the background normalization and is a constant depending on the confidence level ($= 4.6$ for 90% CL contours). If the ν_e contamination is negligible w.r.t. the NC (0) and the ν_e contamination from the beam in the m_{31}^2 region of interest, B is independent of the oscillation parameters. Dropping the m_{31}^2 dependence, the minimum value of $\sin^2 2_{13}$ excluded by the experiment is the one fulfilling:

$$\frac{h}{\frac{(S(\sin^2 2_{13}) + B)}{S_{\text{null}} + B + \frac{2}{2} B^2}} = \frac{(S_{\text{null}} + B)^{i_2}}{(S_{\text{null}} + B)^{i_2}} \quad (11)$$

Assuming complete ignorance on the value of the CP phase and using no other external information to lift the $\sin^2 2_{13}$ ambiguity, the actual excluded $\sin^2 2_{13}$ is

$$\sin^2 2_{13, \text{excl}} = \max_{\sin^2 2_{13}} \sin^2 2_{13, \text{excl}} () \quad (12)$$

In other words, the sensitivity is computed by finding the largest value of $\sin^2 2_{13}$ which is the true $\sin^2 2_{13} = 0$ at the selected confidence level" [17]. If we assume complete ignorance also on the sign of m_{31}^2 the allowed value of $\sin^2 2_{13}$ is the maximum between the value of $\sin^2 2_{13}$ calculated by Eq. 12 assuming $m_{31}^2 > 0$ and the one with $m_{31}^2 < 0$. The expected signal rate in Eq. 10 can be written (see Eq. 5) as:

$$S(\sin^2 2_{13}; \nu) = Y A(\nu) P_{\text{!}}(\sin^2 2_{13}; \nu) \quad (13)$$

and in the narrow beam approximation ($\nu \ll E$ i.)

$$S(\sin^2 2_{13}; \nu) = Y P_{\text{!}}(\sin^2 2_{13}; \nu) \quad (14)$$

where

$$A(\nu) = (E - \nu) \quad (15)$$

Similarly, $S_{\text{null}} = Y P_{\text{!}}(\sin^2 2_{13} = 0; \nu)$ and $B = Y P_{\text{null}}(\nu)$ and $B = Y$, being the background rate per year. Now Eq. 10 reads:

$$P(\sin^2 2_{13}; \nu) > P_{\text{null}}(\nu) + \frac{q - \left(\frac{2}{Y^2} + \frac{2}{2} + \frac{P_{\text{null}}(\nu)}{Y} \right)^{1/2}}{P_{\text{null}}(\nu) + \frac{q - \left(\frac{2}{Y^2} + \frac{2}{2} \right)^{1/2}}{Y^2}}, \quad (16)$$

Exclusion plots for $\sin^2 2_{13}$ are available [7, 15, 16, 27, 28] in the approximation $P(\text{!}) = 0$. This corresponds to the assumption $\nu = 0$ for on-peak experiment ($\nu = 2$) and $\nu = 2$ for off-peak ones ($\nu = 2$). Hence, it is possible to extract the minimum accessible probability P_{min} in:

$$P_{\text{min}} = \frac{q - \left(\frac{2}{Y^2} + \frac{2}{2} \right)^{1/2}}{Y^2} \quad (17)$$

from literature and compute Eq. 16 using the correct oscillation probability⁵. Fig. 3 shows the expected precision for the experiments considered in Sec. 2 for $m_{31}^2 j = 3 \cdot 10^{-3} \text{ eV}^2$ and $m_{21}^2 = 7.3 \cdot 10^{-5} \text{ eV}^2$. The empty boxes indicate the deterioration

⁵The results shown in this sections have been obtained using the complete three family oscillation formula at constant matter density and not the approximate expansion of Eq. 2.

coming from the integration on the CP phase θ . Full boxes show the effect of the sign (m_{31}^2) degeneracy. A few comments are in order. Both JHF-SK and CNGS appear to be almost insensitive to the sign of m_{31}^2 but in fact the effect is subtler. In JHF-SK, the leading term O_1 is independent of the transformation m_{31}^2 ! m_{31}^2 thanks to the smallness of the \hat{A} parameter. O_2 is invariant under this transformation and O_3 is suppressed as well as O_4 . On the other hand, at CNGS the leading term O_1 does not depend significantly on the m_{31}^2 sign thanks to the cancellation of matter effect at work for small values of $j(1 - \hat{A})/j$ (see Sec. 2). The next-to-leading term in the oscillation probability (O_3) is odd under the sign exchange. This effect is equivalent to a $m_{31}^2 \leftrightarrow -m_{31}^2$ transformation so that the same variation of probability appears during the integration in θ ; hence, in Fig. 3 the deterioration of the sensitivity coming from the sign degeneracy is absorbed into the deterioration caused by the CP phase. This different behavior is unveiled examining the exclusion plots at different values of (Fig. 4)⁶. On the other hands, MINOS and NuMI- $\bar{\nu}$ Ax have the highest sensitivity to the m_{31}^2 ! m_{31}^2 transformation since the condition $\hat{A} \neq 0$ affects directly the leading term O_1 . Plots similar to Fig. 3 have already been obtained for JHF and NuMI by the authors of [17] using a detailed simulation of the setups. The bands of Fig. 3 corresponding to these experiments are in good agreement with their results. The CNGS sensitivity has been cross-checked applying the full oscillation probability to the analysis described in [27].

In Sec. 2 we argued that the trade-off between maximal $\sin^2 2\theta_{13}$ sensitivity and maximal PMNS reach is connected with the size of the ratio $m_{21}^2 = j m_{31}^2 j$. Fig. 5 shows the $\sin^2 2\theta_{13}$ sensitivity versus m_{21}^2 for mass ratios up to 10^1 . As expected, the Phase I experiments loose their capability to perform a "pure" $\sin^2 2\theta_{13}$ measurement in the high-LMA region of m_{21}^2 . Note also that the present CHOOZ limit becomes more stringent in the high- m_{21}^2 regime [29].

Fig. 6-a describes the sensitivity in $\sin^2 2\theta_{13}$ versus the integrated flux expressed in years of data taking, assuming the nominal intensity of JHF-SK⁷. The limits have been extracted rescaling naively with \sqrt{Y} the minimum accessible probability P_{min} and ignoring the saturation effect coming from the background normalization. In fact, JHF is expected to be limited by systematics only in the Phase II of its physics program mode. It is worth noting that the deterioration coming from the degeneracies does not imply a plateau of the sensitivity. Phase II experiments will access a region of $\sin^2 2\theta_{13}$ deeper than the one accessible by their Phase I counterparts. As an example in Fig. 6-a the achievable sensitivity on $\sin^2 2\theta_{13}$ after one year data taking of JHF-HK is shown ($m_{21}^2 = 7.3 \times 10^5 \text{ eV}^2$).

After the run, JHF-HK will be able to observe maximal CP violation in the leptonic sector down to $\sin^2 2\theta_{13} \approx 2 \times 10^3$ for $m_{21}^2 \approx 5 \times 10^5 \text{ eV}^2$ [30] and the

⁶Note that for values of $\sin^2 2\theta_{13}$ close to the CHOOZ limit, it could be possible to use synergically JHF-SK and CNGS to get information on the hierarchy of neutrino masses.

⁷It corresponds to a proton intensity of 0.7 MW. Note that 1 year of JHF-HK data taking corresponds to about 125 years of JHF-SK due to the increase of beam intensity and detector mass.

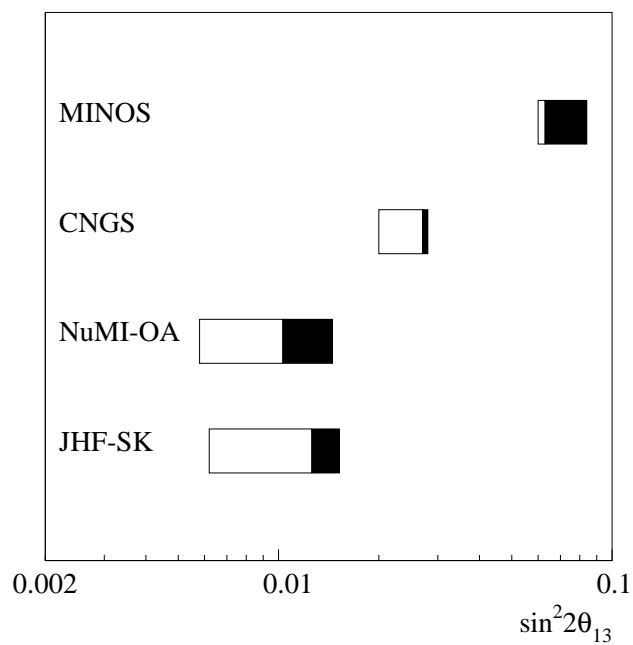


Figure 3: $\sin^2 2\theta_{13}$ sensitivity at 90% CL. Empty boxes correspond to the deterioration due to the ignorance on the phase. Full boxes indicate further deterioration coming from the sign of m_{31}^2 .

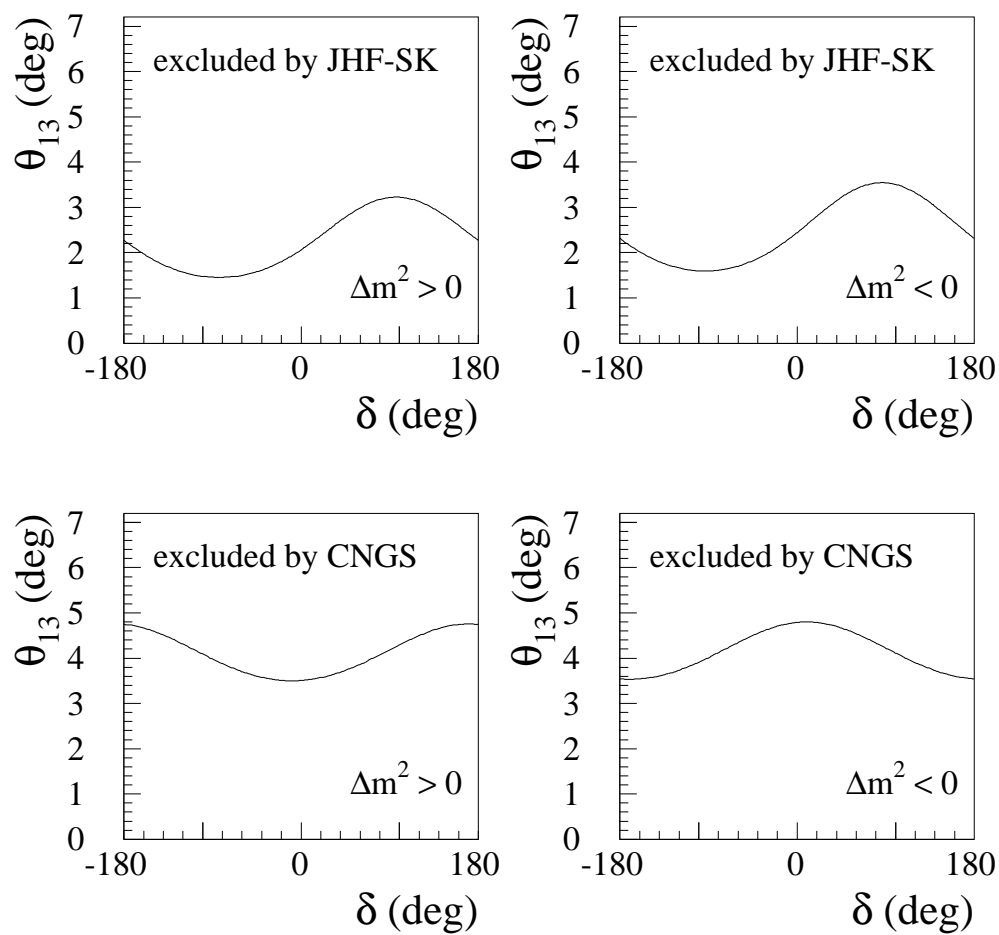


Figure 4: $\sin^2 2 \theta_{13}$ sensitivity at 90% CL versus

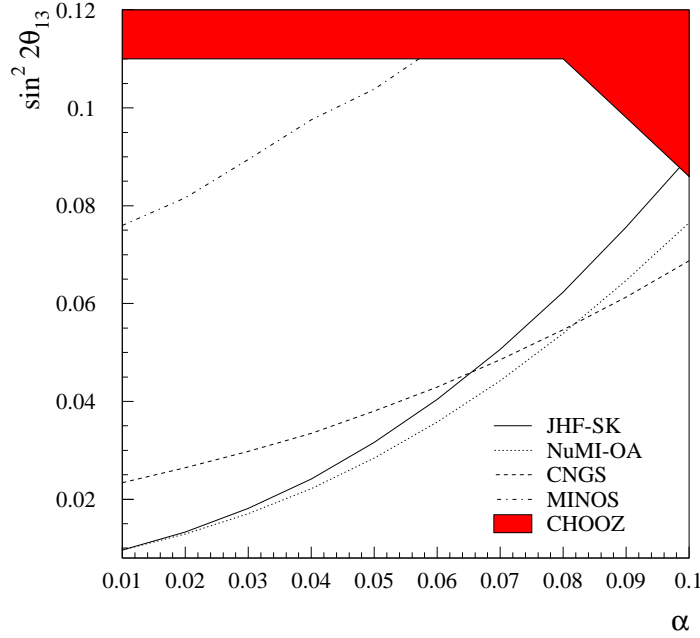


Figure 5: $\sin^2 2\theta_{13}$ sensitivity at 90% CL versus $m_{21}^2 = j m_{31}^2 j$

highest the solar mass, the better the CP-sensitivity (the worse the Phase I "pure" $\sin^2 2\theta_{13}$ sensitivity). So, a null result of JHF-SK cannot rule out convincingly the possibility to perform PMNS precision physics with terrestrial experiments. Of course, this holds also for the Neutrino Factories which have an even higher CP sensitivity than JHF-HK.

Finally, Fig. 6-b shows the $\sin^2 2\theta_{13}$ sensitivity versus the exposure for a CNGS-like beam. For the actual CNGS, the background systematics cannot be neglected. The horizontal lines in the plot indicate the region where the beam systematics will saturate the limits on $\sin^2 2\theta_{13}$ ($B = B_{\text{lim}}$). They correspond to a precision in the normalization of the e background of 10% and 5%. The limit from beam systematics for a setup with a near detector ($\sim 2\%$) is also shown.

4 Conclusions

Phase I experiments will measure the parameters leading the oscillations at the atmospheric scale with unprecedented precision. They will χ the $\sin^2 2\theta_{23}$ and $j m_{31}^2 j$ terms at the 1% level and observe a clear oscillation pattern in disappearance mode. Moreover, they can test the subdominant $e \rightarrow e$ transition improving significantly

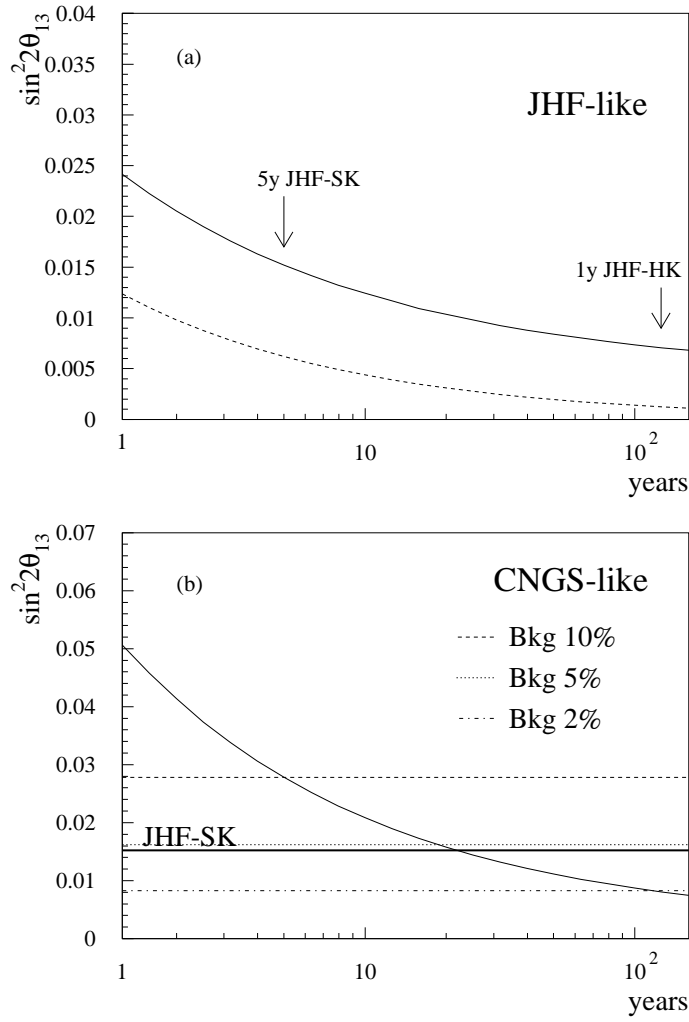


Figure 6: $\sin^2 2\theta_{13}$ sensitivity at 90% CL versus years of exposures for JHF (a) and CNGS (b). In (a) the solid line represents the sensitivity keeping into account the CP phase and $\text{sign}(\sin^2 \theta_{31})$ deterioration. The dashed line shows the expected sensitivity assuming $P(\text{sign}(\sin^2 \theta_{31})) = 0.5$. In (b) the horizontal lines indicate the region where the $\sin^2 2\theta_{13}$ sensitivity becomes limited by the beam systematics (see text).

the present knowledge of $\sin^2 2_{13}$. On the other hand, the actual sensitivity to $\sin^2 2_{13}$ is strongly deteriorated by the present ignorance on the CP violating phase and the sign of m^2_{31} . In Sec. 3 it has been shown that, in case of null result, the improvements in the exclusion limits for $\sin^2 2_{13}$ will be marginal with respect to long baseline experiments like ICARUS and OPERA (0.03 ! 0.015) at $\delta\theta = 0.02$ and negligible for higher values of $\delta\theta$. On the other hand, a high solar scale ($\delta\theta > 0.02$) enhances significantly the capability of Superbeam and Neutrino Factory to access CP violation even for values of $\sin^2 2_{13} = 0 (10^3 - 10^4)$. Hence, a null result at Phase I will not constrain in a significant way the physics reach of SB/NF. Clearly, it is impossible to tune a Phase I experiment to reach simultaneously a high $\sin^2 2_{13}$ sensitivity (setups "ancillary" to Phase II) and a high sensitivity to the CP phase and the mass hierarchy (setups with high "PMNS reach"). At present we do not know if JHF-SK and NuMIO -Axis belong to the former or latter category, due to the large uncertainty on $\delta\theta$. Anyway, a real Phase I experiment (or cluster of experiments) performing a "pure" $\sin^2 2_{13}$ along the line proposed by the authors of [17, 18, 19] would be highly advisable to firmly ground the SB/NF physics programme.

Acknowledgements

We thank A. Donini, M. Lindner and P. Strolin for discussions and careful reading of the manuscript. We are indebted to D. Meloni for providing us with the three family oscillation code and to P. Huber for useful remarks on Eq. 2.

References

- [1] Y. Fukuda et al. [Super-Kamiokande Coll.], Phys. Rev. Lett. 81, 1562 (1998)
M. Ambrosio et al. [MACRO Coll.], Phys. Lett. B 517 (2001) 59
B.T. Cleveland et al., Astrophys. J. 496, 505 (1998)
J.N. Abdurashitov et al. [SAGE Coll.], Phys. Rev. C 60, 055801 (1999)
W. Hampe et al. [GALLEX Coll.], Phys. Lett. B 447, 127 (1999)
S. Fukuda et al. [Super-Kamiokande Coll.], Phys. Rev. Lett. 86, 5651 (2001)
Q.R. Ahmad et al. [SNO Coll.], Phys. Rev. Lett. 87, 071301 (2001).
- [2] M.H. Ahn et al. [K2K Coll.], Phys. Rev. Lett. 90 (2003) 041801.
- [3] K. Eguchi et al. [KamLAND Coll.], Phys. Rev. Lett. 90 (2003) 021802.
- [4] G.L. Fogli, E. Lisi, A. Marrone, D. Montanino, A. Palazzo and A.M. Rotunno, hep-ph/0212127.
- [5] E. Church et al., LA-UR-98-352, Fermilab experiment 898.

[6] E. Ables et al. [MINOS Coll.], FERMILAB-PROPOSAL-P-875
The MINOS detectors Technical Design Report, NuMIL-337, October 1998.

[7] F. Amendo et al. [ICARUS Coll.], ICARUS-TM/2001-08 LNGS-EXP 13/89 add 2/01.

[8] M. Guler et al. [OPERA Coll.], CERN-SPSC-2000-028.

[9] Z. Maki, M. Nakagawa and S. Sakata, Prog. Theor. Phys. 28 (1962) 870
B. Pontecorvo, Sov. Phys. JETP 26 (1968) 984.

[10] See e.g. [30] and references therein.

[11] C. Jarlskog, Phys. Rev. Lett. 55 (1985) 1039.

[12] K. Hagiwara et al., Phys. Rev. D 66 (2002) 010001.

[13] M. Apollonio et al. [CHOOZ Coll.], hep-ex/0301017.

[14] F. Boehm et al. [PALO VERDE Coll.], Phys. Rev. D 64 (2001) 112001.

[15] Y. Itow et al., KEK-REPORT-2001-4, hep-ex/0106019.

[16] D. Ayres et al., hep-ex/0210005.

[17] P. Huber, M. Lindner and W. Winter, hep-ph/0211300.

[18] T. Kajita, H. Minakata and H. Nunokawa, Phys. Lett. B 528 (2002) 245.

[19] H. Minakata et al., hep-ph/0211111.

[20] A. Cervera et al., Nucl. Phys. B 579 (2000) 17, erratum *ibid.* Nucl. Phys. B 593 (2001) 731.

[21] M. Freund, Phys. Rev. D 64 (2001) 053003.

[22] V. Barger, D. Marfatia and K. Whisnant, Phys. Rev. D 65 (2002) 073023.

[23] J. Burguet-Castell et al., Nucl. Phys. B 608 (2001) 301.

[24] J. Burguet-Castell et al., Nucl. Phys. B 646 (2002) 301.
V. Barger, D. Marfatia and K. Whisnant, Phys. Rev. D 66 (2002) 053007.

[25] A. Donini, D. Meloni and P. M. Migliozzi, Nucl. Phys. B 646 (2002) 321.

[26] M. Freund, P. Huber and M. Lindner, Nucl. Phys. B 615 (2001) 331
M. Diwan et al., BNL-69395, hep-ex/0211001.

[27] M. Komatsu, P. M. Migliozzi and F. Terranova, J. Phys. G 29 (2003) 443.

[28] M .D iwan et al., NuM I-NOTE-SIM -0714.

[29] S M .B ilenky, D .N icolo and S.T .Petcov, Phys. Lett. B 538 (2002) 77.

[30] P .Huber, M .Lindner and W .W inter, Nucl. Phys. B 645 (2002) 3.